

## Pulsed Electric Current Sintering and Its Employment for Transparent Polycrystalline $\text{Al}_2\text{O}_3$

Nguyen Huu Hien\* , Makoto Nanko\*\* , Yuzin Xin\* , Takashi Shirai\*\*\*

\*Advanced Ceramics Research Center, Nagoya Institute of Technology  
Gokiso-cho, Showa-ku, Nagoya, Aichi 466-8555, JAPAN

\*\*Department of Mechanical Engineering, Nagaoka University of Technology  
1603-1, Kamitomioka, Nagaoka, Niigata 940-2188, JAPAN

\*\*\*Department of Life Science and Applied Chemistry, Nagoya Institute of Technology  
Gokiso-cho, Showa-ku, Nagoya, Aichi 466-8555, JAPAN

Pulsed electric current sintering (PECS) has become more and more important in material sciences as an advanced method for material fabrication. The remarkable features of PECS in comparison with almost other sintering techniques are the direct heating method and the assistance of pressure. Therefore, PECS has fast heating rate and this sintering technique can densify samples fast without a severe grain growth. The high density and fine microstructure of materials sintered by PECS help a lot in improving properties of materials, especially mechanical properties. Recently, transparent polycrystalline  $\text{Al}_2\text{O}_3$  has attracted much attention among ceramic materials. PECS is a superior sintering method for fabrication of transparent polycrystalline  $\text{Al}_2\text{O}_3$ . This article briefly summarizes the features of PECS and its recent advances in fabrication of transparent polycrystalline  $\text{Al}_2\text{O}_3$ .

**Keyword:** Pulsed electric current sintering, two-step PECS, transparent polycrystalline  $\text{Al}_2\text{O}_3$ , microstructural heterogeneity.

Sintering is one of the excellent methods for shaping of materials. Conventionally, the powder is shaped by pressing in mold in order to form a green body. After that, the green body is sintered by an electrical furnace at high temperature. Conventional sintering showed low ability of densification due to the lack of assistance of pressure. Currently, powder materials can be densified by numerous pressure-assisted sintering techniques such as hot pressing (HP), hot isostatic pressing (HIP) or pulsed electric current sintering (PECS). Among those procedures, HP and HIP methods, which use an indirect heating structure like conventional sintering, often need a long heating time of several hours in order to lead to full densification<sup>[1]</sup>. In contrast, PECS, the latest developed pressure-assisted-sintering process, is a rapid densification process. This feature of PECS not only derives from the support of the uniaxial pressure but also comes from its direct heating method by electrical current. Therefore, it has a big potential to fully densify the powder compact with minimizing grain growth<sup>[2]</sup>.

The schematical design of PECS is showed in Fig. 1. It simultaneously applies an electric pulse along with a uniaxial mechanical pressure in order to sinter the powder compact in a mold set. The applied electric pulse and mechanical pressure can be controlled by a preset

program by controlling the electric current or the in-situ measured temperature.

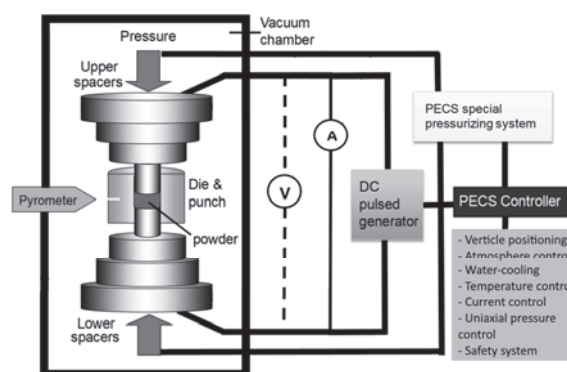


**Fig. 1:** Schematic diagram of pulsed electric current sintering.

In typical PECS methods, powders are poured into a die/punch set and heated by an electric current flowing through the die/punch and powder compact system. Either the powder or the die/punch set or both of them should be electrical conductive in order to guarantee the flow of the electrical current as a close circuit. For the same reason, all of the blocks, including electrodes, spacers, plungers and punches inserted in the circuit (if necessary), should be made of electrical conducting material (stainless steel, graphite, carbides, etc).

Conducting powders are heated both by Joule effect from the current within the powder compact and by heat transfer from the container and electrodes. Otherwise, the non-conductive powders are heated only through the second route. The use of graphite containers, which are mostly applied in the current PECS processes, limits the mechanical pressure levels to low values, generally 100 MPa. In spite of that limitation, the uniaxial pressure of 100 MPa is still high enough to densify in most cases. Therefore, the graphite dies and punches are the most widely used in PECS because of its simple machining. When the ultra high density is required, other materials with stronger mechanical properties can be applied for dies and punches, such as WC or SiC. Grasso et al. used a special design for the mold set of PECS, in which a smaller SiC mold was inserted inside a bigger graphite mold<sup>[3]</sup>, as shown in Fig. 2. With the same design, they could sinter with PECS at a pressure of 500 MPa. Using the same design, Sokol et al. applied 400 MPa or Ratzker et al. applied 800 MPa in their PECS processes<sup>[4,5]</sup>.

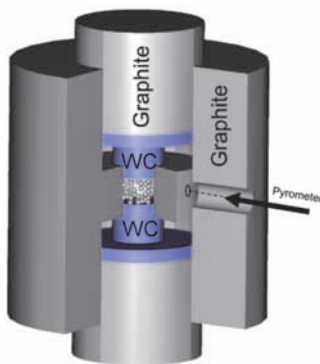


**Fig. 2:** Schematic of the high-pressure SPS device. Reprinted with permission from J. Am. Ceram. Soc., 93 (2010) 2460-2462. Copyright: @ John Wiley and Sons.

The biggest difference of PECS to other pressure-assisted sintering techniques is the application of the electric current through a power supply as the heating source, which leads to a very rapid and efficient heating. The heating rate during the PECS process depends on the geometry of the container and the sample ensemble, its thermal and electrical properties, as well as the electric power supply. Heating rates as high as 100 up to 600°C/min were achieved. In contrast, the typical heating rate of HP or HIP processes is often limited at a few °C/min. As a result, the processing duration of PECS is shortened in compared with HP or HIP processes, which suppresses grain growth in sintering. Hence, the most advantage of PECS processes is the efficient usage

of the heat input, particularly when electrically insulating container is used and the electric current is applied for extremely short duration.

The temperature of PECS process is in-situ measured by a radiation thermometer focused on the surface of the die or by a thermocouple inserted into a hole on the outer surface of the die. The measured temperature at the surface of the die is usually lower than the actual temperature of the sample inside it. Depending on a number of factors such as thermal conductivity of the die and the sample, the heating rate, the applied pressure, the thermal insulation of the die from surrounding, etc, this temperature difference may become quite large. One of the problems of PECS processes is to achieve homogenous temperature distribution in order to achieve a homogeneous sample. In fact, current distribution and consequent temperature distributions within the sample are very sensitive to the homogeneity of the sample after sintering<sup>[6-8]</sup>. The inhomogeneity of temperature in PECS can be considered as its weakness in comparison with other sintering techniques. However, PECS is still used widely to prepare many kinds of materials such as advanced alloy materials, functional gradient materials, advanced ceramics, thermoelectric materials, nano-composites because of its advantages - rapid densification with minimized grain growth.

Aluminum oxide (Al<sub>2</sub>O<sub>3</sub>), commonly referred to alumina, is one of the most widely used engineering ceramic materials, especially its most stable crystalline structure,  $\alpha$ -Al<sub>2</sub>O<sub>3</sub> (or corundum/sapphire). Table 1 lists some of the properties of  $\alpha$ -Al<sub>2</sub>O<sub>3</sub>, which was reported by Doremus<sup>[9]</sup>.

**Table 1:** Physical and mechanical properties of  $\alpha$ -Al<sub>2</sub>O<sub>3</sub>.

Properties	Typical values
Density	3.99 g/cm <sup>3</sup>
Flexural Strength	379 MPa
Compressive Strength	2600 MPa
Hardness (HV)	1440 GPa
Fracture Toughness $K_{IC}$	3 MPam <sup>1/2</sup>
Melting point	2054°C
Thermal Conductivity	35 W/mK
Coefficient of Thermal Expansion	8.4×10 <sup>-6</sup> K <sup>-1</sup>

With high melting point and chemical inertness, Al<sub>2</sub>O<sub>3</sub> is widely used as high-temperature components, catalyst substrates or biomedical implants. Al<sub>2</sub>O<sub>3</sub> is

useful for bearings and cutting tools because of its excellent hardness, strength and good abrasion resistance. Electrical insulators and components are also applications for  $\text{Al}_2\text{O}_3$  based on high electrical resistance. With good optical transparency,  $\text{Al}_2\text{O}_3$  is used as transparent substrates for many optical parts. With the additions of other materials such as graphite, even higher temperatures, harsh environments, and severe applications are envisaged, such as pouring spouts and sliding gate valves at high temperature. For laser host applications, by using ceramic materials, such as  $\text{Al}_2\text{O}_3$ , significantly higher temperatures are potentially attainable.

Pure  $\text{Al}_2\text{O}_3$  is colorless, while the addition of transition metal ions to  $\text{Al}_2\text{O}_3$  creates spectacular colors, gem stones, and practical applications such as ruby lasers.  $\text{Cr}_2\text{O}_3$ -doped  $\text{Al}_2\text{O}_3$ , known as ruby, shows a beautiful red color with about 0.1 mol% of  $\text{Cr}_2\text{O}_3$  [10]. The red color of ruby results from the transitions of electrons between energy levels in its crystal structure. Doping other transition metal ions into  $\text{Al}_2\text{O}_3$  crystals may produce other colors within the range of visible light. For example, the deep blue color is resulted by the addition of a few hundred ppm of  $\text{Fe}^{2+}$  and  $\text{Ti}^{4+}$  impurities [11]. A wide variety of other colors are found in natural and synthetic  $\text{Al}_2\text{O}_3$  crystals. Fig. 3 shows the various colors of transparent  $\text{Al}_2\text{O}_3$  and  $\text{MgAl}_2\text{O}_4$  ceramics, fabricated by adding an amount of transition metal ions and sintering by PECS.

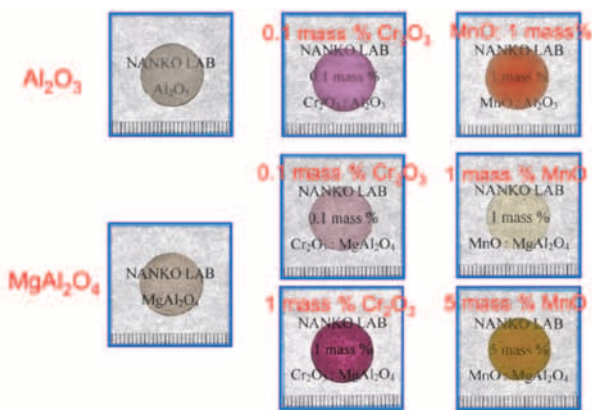


**Fig. 3:** Appearance of various transparent  $\text{Al}_2\text{O}_3$  and  $\text{MgAl}_2\text{O}_4$  added with different dopants. Reprinted with permission. Copyright: © 2015 Nanko M, Dang KQ. Published in [Pulsed electric current sintering of transparent alumina ceramics, in "Sintering techniques of materials", InTech] under CC BY 3.0 license. Available from: <http://dx.doi.org/10.5772/59170>.

In preparation of transparent polycrystalline  $\text{Al}_2\text{O}_3$ ,

the two most important factors are density and grain size [3, 12-40]. Due to the negative influences of pores on the optical transparency, transparent polycrystalline materials requires extremely low porosity (<0.01 vol%) [18, 20, 21, 37]. It is also believed that polycrystalline materials with nano-scaled grain size would provide better transparency than materials with a grain size in the micrometric range. Moreover, the nano-scaled grain size of the polycrystalline matrix also accommodates with significant improvement in the mechanical properties. Traditional transparent polycrystalline  $\text{Al}_2\text{O}_3$  are prepared by sintering in hydrogen gas at temperature generally above  $1700^\circ\text{C}$  [13, 41]. That high sintering temperature produces polycrystalline  $\text{Al}_2\text{O}_3$  with low porosity but causes extensive grain growth, which dramatically reduces the mechanical strength, hardness and optical transparency of the material. As a result, the optical in-line transmission of polycrystalline  $\text{Al}_2\text{O}_3$  produced by conventional sintering is typically below 10%, and the material appears translucent rather than transparent [14]. This matter obviously indicates that conventional sintering is not appropriate to produce transparent polycrystalline  $\text{Al}_2\text{O}_3$ .

Currently, fine-grained transparent  $\text{Al}_2\text{O}_3$  have been successfully prepared by HP, HIP or PECS at a low temperature range, from  $1150$  to  $1400^\circ\text{C}$  [15, 18-20]. By HP or HIP techniques, the sample is heated by the heat transfer from the external surface of the container to the powder compacts. The consequent heating rate is then typically slow, as lower as  $10^\circ\text{C}/\text{min}$  and the process normally lasts for hours. The long process at high temperature causes serious grain growth, which is unfavorable for fabrication of transparent  $\text{Al}_2\text{O}_3$ . The large grain size of  $\text{Al}_2\text{O}_3$  bulks leads to the reduction of the optical inline transmittance and the mechanical properties, such as hardness, fracture toughness or abrasion resistance [21, 22, 26]. The common strategy for sintering of transparent polycrystalline  $\text{Al}_2\text{O}_3$  is to improve the densification without significant grain growth. The fine-grained microstructure ( $< 1 \mu\text{m}$ ) provides polycrystalline  $\text{Al}_2\text{O}_3$  with a significant improvement in both mechanical strength and optical transparency. It is reported that bending strength of the fine-grained transparent  $\text{Al}_2\text{O}_3$  is up to  $400$ - $600$  MPa with a high in-line transmission up to 60% for visible light [14, 26]. The addition of  $\text{MgO}$  is well-known to annihilate normal and abnormal grain growth during sintering of polycrystalline  $\text{Al}_2\text{O}_3$  [16, 25]. As the result,

polycrystalline Al<sub>2</sub>O<sub>3</sub> has finer microstructure in grain size with higher final density.

Recently, PECS has become an alternative method to fabricate transparent polycrystalline Al<sub>2</sub>O<sub>3</sub> [3, 15-20, 37-41]. It is reported by Kim et al. [19] and Dang et al. [38, 39] that a slow heating rate, such as 2°C/min, was the critical PECS parameter for densification of transparent Al<sub>2</sub>O<sub>3</sub> prepared by PECS. Grasso et al. reported that a high pressure of 500 MPa promoted densified and transparent Al<sub>2</sub>O<sub>3</sub> in PECS at low temperature of 1000°C [3]. Langer et al. reported about comparison between HP and PECS processing for the Al<sub>2</sub>O<sub>3</sub> powder (TM-DAR). By fixing the sample geometry, the heating program, the applied pressure and the atmosphere for both sintering processes, at a given constant time, PECSed samples achieved higher relative density than HPed ones [42].

In consideration of the most impressive advantage of PECS as the high heating rate, Nanko et al. established a new technique with PECS to prepare polycrystalline Al<sub>2</sub>O<sub>3</sub> with high transparency: two-step PECS (TS-PECS) [37]. Fig. 4 shows the comparison of some common temperature programs of the PECS processes. A normal one-step PECS process with high heating rate, indicated as the line no. 1, was used commonly but resulted in an opaque or translucent polycrystalline Al<sub>2</sub>O<sub>3</sub> samples. To obtain transparent polycrystalline Al<sub>2</sub>O<sub>3</sub>, the one-step PECS program, which is indicated as line no. 2, employed a much slower heating rate, such as 2°C/min, leading to high density with small grain size [19]. TS-PECS was established with two stages of temperature holding.

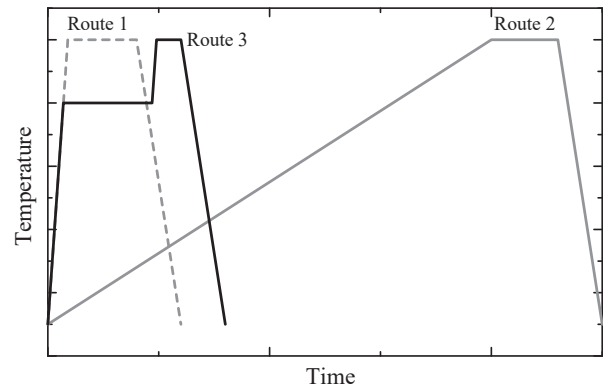


**Fig. 4:** PECS temperature programs: (1) Normal PECS with high heating rate, (2) Normal PECS with low heating rate, (3) TS-PECS with high heating rate.

Instead of slowly heating up to the final sintering temperature, a holding stage with lower temperature was applied for partial densification without serious grain growth. After that, the temperature was risen to the final sintering temperature to complete densification with preserving the grain size. In both two steps of heating up, the heating rate was 100°C/min [37]. By using TS-PECS, polycrystalline Al<sub>2</sub>O<sub>3</sub> with comparatively high transparency was fabricated in a shorter total time than by using a normal PECS process with low heating rate.

Otherwise, Grasso et al. used PECS with two-step pressure pattern to improve the transparency of polycrystalline Al<sub>2</sub>O<sub>3</sub> [43]. Fig. 5 shows their Al<sub>2</sub>O<sub>3</sub> samples densified with two PECS pattern: constant pressure and two-step pressure. Based on the consideration that the heterogeneous densification was

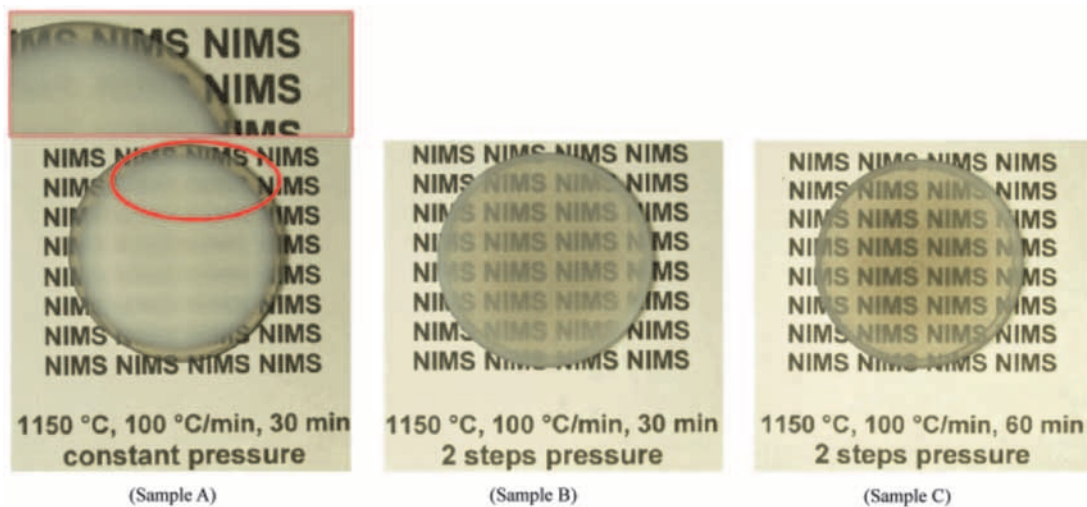


**Fig. 5:** Photograph of alumina ceramics disks sintered by SPS at 1150°C with a heating rate of 100°C/min. The sample shown in figure (a) was sintered for 30 min under 80 MPa constant pressure. The sample (b) and (c) were sintered with pressure two steps pressure application for 30 and 60 min. The samples are 3 cm in diameter and are on top of the text. Reprinted with permission from J. Am. Ceram. Soc., 94 [5] (2011), 1405–1409. Copyright: © John Wiley and Sons.

the reason for the heterogeneous transparency, they applied low pressure (35 MPa) before the dwelling stage to slow down the densification of the sample's border at the beginning, consequently leading to a more uniform densification at the final stage with higher pressure (80 MPa).

As transparent  $\text{Al}_2\text{O}_3$  has been a remarkable material in industries, there are a huge amount of publications on transparent polycrystalline  $\text{Al}_2\text{O}_3$  fabricated by PECS. However, almost of the polycrystalline  $\text{Al}_2\text{O}_3$  with high transparency fabricated by PECS were sintered at small and thin size, such as 15 mm in diameter or even smaller. The disadvantage of PECS is that there is always a heterogeneity distribution of temperature and pressure inside the powder compact. At small size, this heterogeneity should be not severe but it may be more serious at larger sizes. Among many ceramic materials, transparent polycrystalline  $\text{Al}_2\text{O}_3$  is a temperature-sensitive material. If the temperature increases just a little, the grain growth may occur seriously and reduce the optical transparency. Because of this characteristic of the PECS process and the strict requirements of transparent polycrystalline  $\text{Al}_2\text{O}_3$ , this material fabricated by PECS is often limited on sintering size. For larger sizes, there have been many reports on the heterogeneity of the transparent polycrystalline  $\text{Al}_2\text{O}_3$  samples produced by PECS [3, 12, 15, 17-20, 37, 40, 43-45]. Roussel et al. showed their polycrystalline  $\text{Al}_2\text{O}_3$  samples with a diameter of 20 mm [44]. Their samples were transparent in the center but translucent at the edge and the optical transmittance was improved by using La dopant, as shown in Fig. 6. However, there was no discussion on that heterogeneity of polycrystalline  $\text{Al}_2\text{O}_3$  samples. Grasso et al. reported a reverse situation about heterogeneity of sintered  $\text{Al}_2\text{O}_3$  samples with a diameter of 30 mm. The border of sample was denser, had smaller grain size and was transparent while the center was opaque [43]. Wang et al. reported the heterogeneity of grain size of polycrystalline  $\text{Al}_2\text{O}_3$  samples with various diameters from 12 to 50 mm [46]. Regardless of the differences in grain size at different positions along the radial axis of the samples, the grain size at corresponding positions between various samples was totally different, even the sintering conditions were the same for all of  $\text{Al}_2\text{O}_3$  samples with various diameters. This heterogeneity of the polycrystalline  $\text{Al}_2\text{O}_3$  samples derived from the heterogeneous distribution of the sample temperature and pressure during PECS processes. The difficulty of controlling the distribution

of temperature and pressure during sintering processes by PECS causes the difficulty of sintering large-sized specimens. Some studies on simulation of PECS processes by finite element method (FEM) reported the heterogeneous distribution of the temperature during PECS processes [46-48]. In almost cases, the distribution of temperature was reported more heterogeneously with the larger sintering size. Therefore, sintering of large-sized transparent polycrystalline  $\text{Al}_2\text{O}_3$  by PECS is still a challenge.

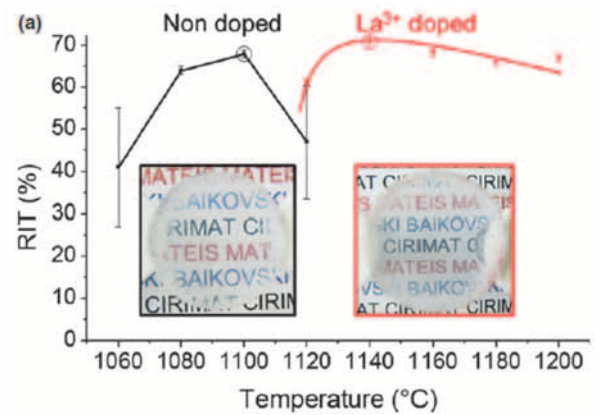


**Fig. 6:** Dependence of sintering temperature on the real inline transmittance of nondoped and  $\text{La}^{3+}$ -doped sintered  $\alpha\text{-Al}_2\text{O}_3$ , showing a larger range of densification temperatures with  $\text{La}^{3+}$  dopant. Reprinted with permission from J. Am. Ceram. Soc., 96 [4] (2013), 1039–1042. Copyright: @John Wiley and Sons.

In our studies of TS-PECS, the transparent polycrystalline  $\text{Al}_2\text{O}_3$  samples with a diameter of 30 mm were successfully fabricated by the combination of two strategies: the optimization of sintering parameters and the usage of dopants. The sintering temperature of TS-PECS program was  $930^\circ\text{C}$  for the first soaking step and  $1130^\circ\text{C}$  for the second one. In order to decrease the heterogeneity of grain size of polycrystalline  $\text{Al}_2\text{O}_3$  samples, the slow heating rate, such as  $10^\circ\text{C}/\text{min}$ , was applied.

The commercial high-purity  $\text{Al}_2\text{O}_3$  powder (Taimei Chemicals, TM-DAR) was sintered by TS-PECS with three temperature patterns at the same heating rate of  $100^\circ\text{C}/\text{min}$ . The heterogeneity of grain size of those three samples was shown in Fig. 7a. The  $\text{Al}_2\text{O}_3$  sample sintered at  $900\text{--}1100^\circ\text{C}$  had the smallest and most homogeneous grain size but low relative density, at 99.6%. Due to its low transparency, that sample was not further investigated. On the other hand,  $\text{Al}_2\text{O}_3$  sample sintered at  $950\text{--}1150^\circ\text{C}$  obtained higher density, at 99.8%, but was opaque because of the large grain size.

Therefore, the sintering temperature pattern of 930-1130°C was chosen to conduct further investigation of the heating rate. In Fig. 7b, the heating rate was reduced from 100 to 40 and 10°C/min and the relative density of those three samples were 99.8, 99.9 and 99.9%, correspondingly. With decreasing of the heating rate, the grain size of polycrystalline Al<sub>2</sub>O<sub>3</sub> sintered by TS-PECS method became smaller and more homogeneous. The apparent optical transmittance of those three samples is shown in Fig. 8, where the optical transmittance was highest with the lowest heating rate, at 10°C/min. However, the optical transmittance of that sample reduced at the edge of the sample. The appearance of the three samples also showed the consistence with the results of optical transmittance. The grain size at the center was larger than near the edge, which typically led to a lower optical transmittance at the center of the sample. In this result, the lower optical transmittance at the edge of the sample was supposed to indicate a heterogeneity of density or porosity of the sample. Unfortunately, the relative density of the samples was almost 99.9-100% and the common Archimedes's method is not accurate enough to detect the difference in relative density at the level of 0.01%. The reasons of the heterogeneous transparency in this case were still unknown and need further studying in the future.

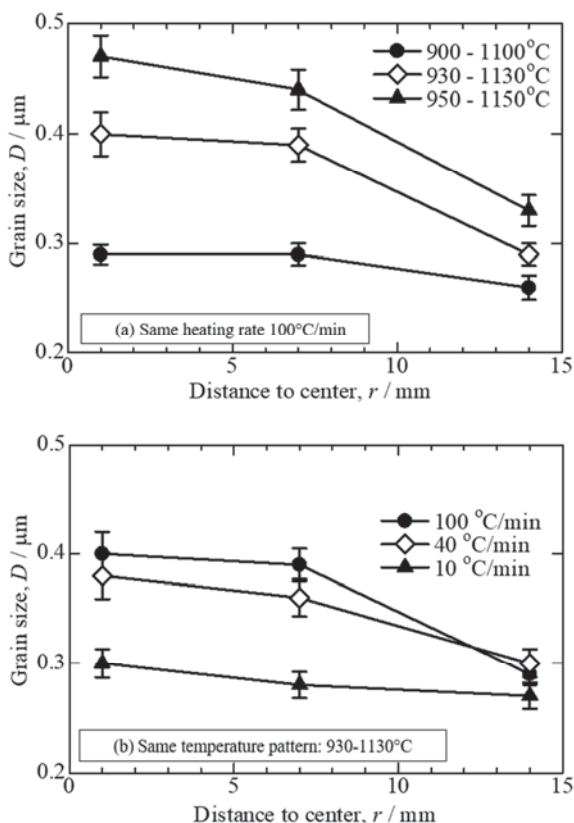


**Fig. 7:** Distribution along the radial axis of grain size of polycrystalline Al<sub>2</sub>O<sub>3</sub> samples with different sintering parameters.

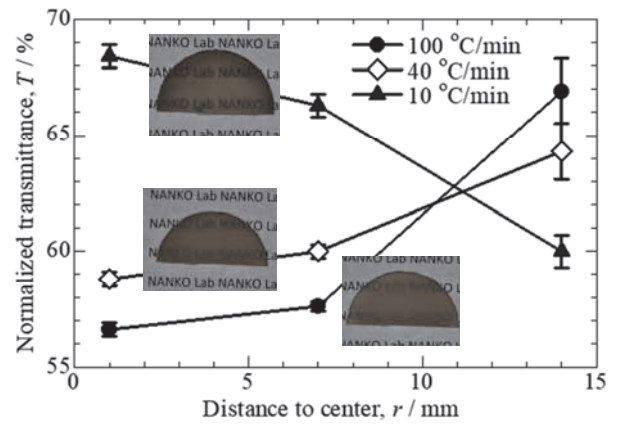


**Fig. 8:** Apparent optical transmittance of polycrystalline Al<sub>2</sub>O<sub>3</sub> samples sintered by TS-PECS with different heating rate.

With the optimization of the temperature and heating rate of TS-PECS program, the large-sized transparent polycrystalline Al<sub>2</sub>O<sub>3</sub> was fabricated with good transparency and significantly homogeneous grain size. However, there was still a heterogeneity of the optical transmittance along the radial axis of the transparent bulk samples.

The other routes to control the fine and homogeneous microstructure of the polycrystalline Al<sub>2</sub>O<sub>3</sub> are using dopants. Some studies reported that the usage of dopants could slow down the grain growth behavior of the polycrystalline Al<sub>2</sub>O<sub>3</sub> during sintering process, so that the fine microstructure could be preserved after sintering [17, 44, 47, 49-53]. One of the most common dopants to reduce grain growth rate of polycrystalline Al<sub>2</sub>O<sub>3</sub> was MgO. The influences of MgO dopant in controlling microstructure of polycrystalline Al<sub>2</sub>O<sub>3</sub> were reported by Wang et al. [47] and Stuer et al. [17]. Besides MgO, Stuer also used Y and La as the dopants and they reported that the triple doping of Mg-Y-La gave the best results in decreasing the grain size and consequently increasing the optical transmittance of polycrystalline Al<sub>2</sub>O<sub>3</sub>. Voytovych et al. reported that yttrium doping inhibited both densification and coarsening of sintered  $\alpha$ -Al<sub>2</sub>O<sub>3</sub> at 1450°C [52]. The influences in densification behavior were suggested relating to the transition from grain boundary diffusion to lattice diffusion controlled densification with increasing temperature. Bojarski et al. also reported a similar influence of Y and La co-doping on the grain growth behavior of Al<sub>2</sub>O<sub>3</sub> [51]. Yoshida et al. investigated the densification of Ti-doped Al<sub>2</sub>O<sub>3</sub> and showed that the densification and grain growth of Al<sub>2</sub>O<sub>3</sub> sintered in N<sub>2</sub>+H<sub>2</sub> gas atmosphere was depressed by Ti dopant [54].

**Table 2: Sintering temperature of TS-PECS of undoped and doped polycrystalline  $\text{Al}_2\text{O}_3$  samples, and relative density of sintered bodies.**

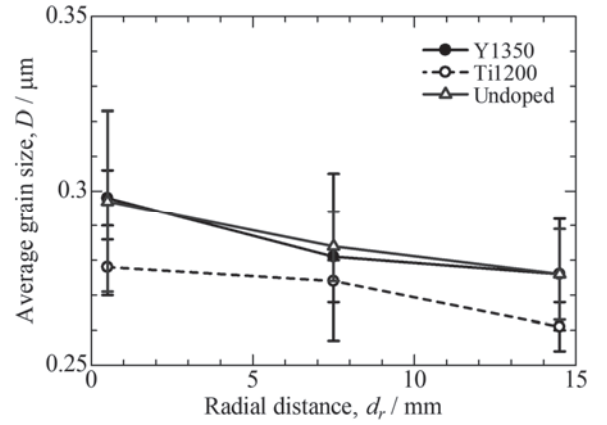
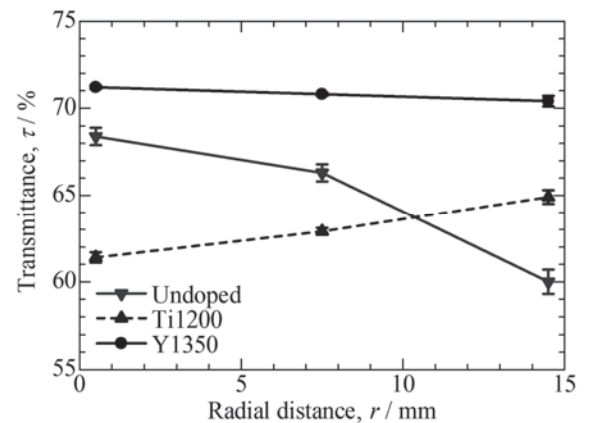
Dopant	Sintering temperature 1 <sup>st</sup> – 2 <sup>nd</sup> step	Annotation	Relative density	Notes
-	930-1130°C	Undoped	99.9%	Transparent - White
<b>TiO<sub>2</sub></b> <b>(0.1 mol%)</b>	930-1130°C	Ti1130	98.1%	Opaque
	1000-1200°C	Ti1200	99.9%	Transparent - Dark
<b>Y<sub>2</sub>O<sub>3</sub></b> <b>(0.1 mol%)</b>	930-1130°C	Y1130	80.6%	Opaque
	1000-1200°C	Y1200	92.8%	Opaque
	1100-1300°C	Y1300	99.8%	Translucent
	1150-1350°C	Y1350	99.9%	Transparent - White

Trunec et al. also successfully reduced the grain size as well as improved the optical transparency of polycrystalline  $\text{Al}_2\text{O}_3$  by using zirconia-spinel co-doping with a combination of PECS and HIP [49].

In our own study, the microstructure of polycrystalline  $\text{Al}_2\text{O}_3$  was controlled by using two dopants,  $\text{TiO}_2$  and  $\text{Y}_2\text{O}_3$ . With both dopants, the densification and grain growth of polycrystalline  $\text{Al}_2\text{O}_3$  were depressed. However, the influences of  $\text{Y}_2\text{O}_3$  dopant was much stronger than  $\text{TiO}_2$ . The influences of Ti and Y dopants in densification of polycrystalline  $\text{Al}_2\text{O}_3$  can be seen obviously in Table 2. While the undoped  $\text{Al}_2\text{O}_3$  was fully densified at the sintering temperature of 930-1130°C for TS-PECS, the Ti-doped and Y-doped ones required 1000-1200°C and 1150-1350°C, respectively, for fully densification.

Fig. 9 shows the distribution of grain size of transparent samples along the radial axis. Even at much higher sintering temperature, 1150 and 1350°C for the two steps, the grain size of  $\text{Y}_2\text{O}_3$ -doped  $\text{Al}_2\text{O}_3$  sample was still equivalent with that of the undoped ones. The grain size of  $\text{TiO}_2$ -doped  $\text{Al}_2\text{O}_3$  was a bit smaller than the undoped one, although the sintering temperature was a bit higher. Both results indicated that the dopants dramatically depressed the grain growth of polycrystalline  $\text{Al}_2\text{O}_3$ . Fig. 10 shows the apparent optical transmittance of the three transparent samples, measured at different positions along the radial axis. Although the detailed understanding of the heterogeneity of optical transmittance has been still not clear yet, the results showed obviously that the dopant of  $\text{Y}_2\text{O}_3$  could improve optical transparency of polycrystalline  $\text{Al}_2\text{O}_3$  as well as its homogeneity. It indicated that the additive of  $\text{Y}_2\text{O}_3$  dopant is excellent to control the microstructure of polycrystalline  $\text{Al}_2\text{O}_3$ . Although  $\text{TiO}_2$  dopant could depress the grain growth of polycrystalline  $\text{Al}_2\text{O}_3$  and improve the homogeneity of grain size, it caused a dark

color for polycrystalline  $\text{Al}_2\text{O}_3$  samples, which led to a significantly lower optical transmittance. Therefore, the  $\text{TiO}_2$  dopant is not good for transparent polycrystalline  $\text{Al}_2\text{O}_3$ .


**Fig. 9:** Distribution along the radial axis of grain size of polycrystalline  $\text{Al}_2\text{O}_3$  samples with different dopants.

**Fig. 10:** Apparent optical transmittance of polycrystalline  $\text{Al}_2\text{O}_3$  samples sintered by TS-PECS with different dopants and corresponding sintering temperature.

In summary, PECS has been used widely to fabricate transparent polycrystalline  $\text{Al}_2\text{O}_3$ . However, the optical transparency of polycrystalline  $\text{Al}_2\text{O}_3$  is still not

as good as single crystal sapphire, which has been applied in many industries for many years. The necessary improvements for transparent polycrystalline Al<sub>2</sub>O<sub>3</sub> includes the optical transparency, the homogeneity of the sintered bodies as well as the sintering size. Along with the developments of PECS and its related sintering methods, polycrystalline Al<sub>2</sub>O<sub>3</sub> is expected to substitute single crystal one in variety of industrial applications.

### References

- [1] M. Nanko, "High gas pressure processed to obtain tailored porous materials and perfect spheres", Ph.D. Dissertation, Nagaoka University of Technology, Japan, 1994.
- [2] M. Tokita, "Trends in advanced SPS spark plasma sintering systems and technology", J. Soc. Powder Technol. Jpn., 30 (1993) 790-804.
- [3] S. Grasso, B. N. Kim, C. Hu, G. Maizza and Y. Sakka, "Highly transparent pure alumina fabricated by high-pressure spark plasma sintering", J. Am. Ceram. Soc., 93 (2010) 2460-2462.
- [4] M. Sokol, S. Kalabukhov, M. P. Dariel and N. Frage, "High-pressure spark plasma sintering (SPS) of transparent polycrystalline magnesium aluminate spinel (PMAS)", J. Eur. Ceram. Soc., 34 (2014) 4305-4310.
- [5] B. Ratzker, A. Wagner, M. Sokol, S. Kalabukhov and N. Frage, "Stress-enhanced dynamic grain growth during high-pressure spark plasma sintering of alumina", Acta Mater. 164 (2019), 390-399.
- [6] K. Matsugi, H. Kuramoto, T. Hatayama and O. Yanagisawa: "Temperature distribution at steady state under constant current discharge in spark sintering process of Ti and Al<sub>2</sub>O<sub>3</sub> powders", J. Mater. Proc. Tech. 134 (2003) 225-232.
- [7] Y. C. Wang, Z. Y. Fu, W. M. Wang and H. X. Zhu, "Temperature field distribution in spark plasma sintering of BN", J. Wuhan Univ. Tech. 17 (2002), 19-21.
- [8] Y. Wang, Z. Fu and Q. Zhang, "SPS temperature distribution of different conductivity materials", Key Engineering Materials 224-226 (2002) 717-720.
- [9] R.H. Doremus, Chapter 1 – Alumina, in J. F. Shackelford and R.H. Doremus (Ed.), "Ceramic and glass materials: Structure, properties and processing" (pp 1-26), Springer, New York, USA, 2008.
- [10] M. Nanko and Q. K. Dang (2015), Pulsed electric current sintering of transparent alumina ceramics, in "Sintering techniques of materials", InTech.
- [11] S. K. Shevell, "The science of color", Elsevier, Oxford, UK, 2003.
- [12] Q. K. Dang, "Pulsed electric current sintering of  $\alpha$ -Al<sub>2</sub>O<sub>3</sub> powder to fabricate transparent bodies", Ph.D. Dissertation, Nagaoka University of Technology, Japan, 2010.
- [13] X. J. Mao, S. W. Wang, S. Shimai and J. K. Guo, "Transparent Polycrystalline Alumina Ceramics with Orientated Optical Axes", J. Am. Ceram. Soc., 91 (2008) 3431-3.
- [14] H. Mizuta, K. Oda, Y. Shibasaki, M. Maeda, M. Machida and K. Ohshima, "Preparation of High-Strength and Translucent Alumina by Hot Iso-Static Pressing", J. Am. Ceram. Soc., 75 (1992) 469-73.
- [15] D. Jiang, D. M. Hulbert, U. Anselmi-Tamburini, T. Ng, D. Land and A. K. Mukherjee, "Optically transparent polycrystalline Al<sub>2</sub>O<sub>3</sub> produced by spark plasma sintering", J. Am. Ceram. Soc., 91 (2008) 151-154.
- [16] M. Suárez, A. Fernández, J.L. Menéndez and R. Torrecillas, "Grain growth control and transparency in spark plasma sintered self-doped alumina materials", Scripta Mater., 61 (2009) 931-934.
- [17] M. Stuer, Z. Zhao, U. Aschauer and P. Bowen, "Transparent polycrystalline alumina using spark plasma sintering: Effect of Mg, Y and La doping", J. Eur. Ceram. Soc., 30 (2010) 1335-1343.
- [18] B. N. Kim, K. Hiraga, K. Morita and H. Yoshida, "Spark plasma sintering of transparent alumina", Scripta Mater., 57 (2007) 607-610.
- [19] B. N. Kim, K. Hiraga, K. Morita and H. Yoshida, "Effects of heating rate on microstructure and transparency of spark plasma sintered alumina", J. Eur. Ceram. Soc., 29 (2009) 323-327.
- [20] B. N. Kim, K. Hiraga, K. Morita, H. Yoshida, T. Miyazaki and Y. Kagawa, "Microstructure and optical properties of transparent alumina", Acta. Mater., 57 (2009) 1319-1326.
- [21] R. Apetz and M. P. B. Bruggen, "Transparent alumina: A light-scattering model", J. Am. Ceram. Soc. 86 (2003) 480-486.
- [22] Y. T. O, J. Koo, K. J. Hong, J. S. Park and D. C. Shin, "Effect of grain size on transmittance and mechanical strength of sintered alumina", Mater. Sci. Eng. A., 374 (2004) 191-195.
- [23] C. Pecharromàn, G. Mata-Osoro, L. Antonio Diaz, R. Torrecillas and J.S. Moya, "On the transparency of nanostructured alumina: Rayleigh-Gans model for anisotropic spheres", Opt. Express, 17 (2009), 6899-6912.
- [24] A. Braun, G. Falk and R. Clasen, "Transparent polycrystalline alumina ceramic with sub-micrometre microstructure by means of electrophoretic deposition", Mater. Wiss. Werkst., 37 (2006) 293-297.
- [25] G. Bernard-Granger and C. Guizard, "Influence of MgO or TiO<sub>2</sub> doping on the sintering path and on the optical

- properties of a submicronic alumina material”, *Scripta Mater.*, 56 (2007) 983-986.
- [26] A. Krell, P. Blank, H. Ma and T. Hutzler, “Transparent sintered corundum with high hardness and strength”, *J. Am. Ceram. Soc.*, 86 (2003) 12-18.
- [27] A. Krell and J. Klimke, “Effects of the homogeneity of particle coordination on solid-state sintering of transparent alumina”, *J. Am. Ceram. Soc.*, 89 (2006) 1985-1992.
- [28] D. S. Kim, J. H. Lee, R. J. Sung, S. W. Kim, H. S. Kim and J. S. Park, “Improvement of translucency in  $\text{Al}_2\text{O}_3$  ceramics by two-step sintering technique”, *J. Eur. Ceram. Soc.*, 27 (2007) 3629-3632.
- [29] J. Cheng, D. Agarwal, Y. Zhang, and R. Roy, “Microwave sintering of transparent alumina”, *Mater. Lett.*, 56 [4] (2002) 587-92.
- [30] O. H. Kwon, C. S. Nordahl, and G. L. Messing, “Submicrometer transparent alumina by sinter forging seeded  $\gamma$ -alumina powders”, *J. Am. Ceram. Soc.*, 78 (1995) 491-4.
- [31] R. L. Coble, “Transparent alumina and method of preparation”, U.S. Patent No. 3,026,210 (1962).
- [32] J. G. J. Peelen, “Light transmission of sintered alumina”, *Philips Tech. Rev.*, 36 (1976) 47-52.
- [33] J. G. J. Peelen, “Transparent hot-pressed alumina. I: Hot pressing of alumina”, *Ceramurgia Intl.*, 5 (1979) 70-75.
- [34] J. G. J. Peelen, “Transparent hot-pressed alumina. II: Transparent versus translucent alumina”, *Ceramurgia Intl.*, 5 (1979) 115-119.
- [35] K. Hayashi, O. Kobayashi, S. Toyoda and K. Morinaga, “Transmission optical properties of polycrystalline alumina with submicron grains”, *Mater. Trans, JIM*, 32 (1991) 1024-1029.
- [36] Y. Aman, V. Garnier and E. Djurado, “A screening design approach for the understanding of spark plasma sintering parameter: A case of translucent polycrystalline undoped alumina”, *Int. J. Appl. Ceram. Technol.*, 7 (2010) 574-586.
- [37] M. Nanko and Q. K. Dang, “Two-step pulsed electric current sintering of transparent  $\text{Al}_2\text{O}_3$  ceramics”, *Advances in Applied Ceramics* 113 (2014) 80-84.
- [38] K. Q. Dang and M. Nanko, “Transparent Cr-doped  $\text{Al}_2\text{O}_3$  made by Pulsed Electric Current Sintering Process”, *Advances in Technology of Materials and Materials Processing Journal*, 12 [1] (2010), 19-24.
- [39] K. Q. Dang, S. Takei, M. Kawahara and M. Nanko, “Pulsed Electric Current Sintering of Transparent Cr-doped  $\text{Al}_2\text{O}_3$ ”, *Ceramic International*, 37 [3] (2011), 957-963.
- [40] H. H. Nguyen, M. Nanko and K. Q. Dang, “Reduction of black dots in transparent polycrystalline alumina produced by pulsed electric current sintering with various chemical powder treatments”, *J. Ceram. Soc. Japan* 124 (2016) 354-359.
- [41] G. C. Wei and W. H. Rhodes, “Sintering of Translucent Alumina in a Nitrogen–Hydrogen Gas Atmosphere”, *J. Am. Ceram. Soc.*, 83 (2000) 1641-8.
- [42] J. Langer, M. J. Hoffmann and O. Guillon, “Direct Comparison Between Hot Pressing and Electric Field-Assisted Sintering of Submicron Alumina”, *Acta Mater.*, 57, (2009) 5454–5465.
- [43] S. Grasso, C. Hu, G. Maizza, B. N. Kim and Y. Sakka, “Effects of pressure application method on transparency of spark plasma sintered alumina”, *J. Am. Ceram. Soc.*, 94 [5] (2011), 1405–1409.
- [44] N. Roussel, L. Lullemant, J. Y. C. Ching, S. G. Frisch, B. Durand, V. Garnier, G. Bonnefont, G. Fantozzi, L. Bonneau, S. Trombert and D. G. Gutierrez, “Highly dense, transparent  $\alpha$ - $\text{Al}_2\text{O}_3$  ceramics from ultrafine nanoparticles via a standard SPS sintering”, *J. Am. Ceram. Soc.*, 96 [4] (2013), 1039–1042.
- [45] X. Jin, L. Gao and J. Sun, “Highly transparent alumina spark plasma sintered from common-grade commercial powder: The effect of powder treatment”, *J. Am. Ceram. Soc.*, 93 [5] (2010), 1232–1236.
- [46] C. Wang, L. Cheng and Z. Zhao, “FEM analysis of the temperature and stress distribution in spark plasma sintering: Modelling and experimental validation”, *Computational Materials Science*, 49 (2010), 351-362.
- [47] C. Wang, X. Wang and Z. Zhao, “Microstructure homogeneity control in spark plasma sintering of  $\text{Al}_2\text{O}_3$  ceramics”, *J. Eur. Ceram. Soc.*, 31 (2011), 231-235.
- [48] N. Maruyama and W. Shin, “Effect of rapid heating on densification and grain growth in hot pressed alumina”, *J. Ceram. Soc. Japan* 108 (2000), 799-802.
- [49] M. Trunec, J. Klimke and Z. J. Shen, “Transparent alumina ceramics densified by a combination approach of spark plasma sintering and hot isostatic pressing”, *J. Eur. Ceram. Soc.*, 36 (2016) 4333-4337.
- [50] P. Liu, H. Yi, G. Zhou J. Zhang and S. Wang, “HIP and pressureless sintering of transparent alumina shaped by magnetic field assisted flip casting”, *Optical Materials Express*, 5 (2015), 441-446.
- [51] S. A. Bojarski, M. Stuer, Z. Zhao, P. Bowen and S. Gregory, “Influence of Y and La additions on grain growth and the grain-boundary character distribution of alumina”, *J. Am. Ceram. Soc.*, 97 (2014), 622-630.
- [52] R. Voytovych, I. MacLaren, M. A. Gulgun, R. M. Cannon and M. Ruhle, “The effect of yttrium on densification and grain growth in  $\alpha$ -alumina”, *Acta Materialia*, 50 (2002), 3453-3463.

- [53] A. S. A. Chinelatto, E. M. J. A. Pallone, A. M. Souza, M. K. Manosso, A. L. Chinelatto and R. Tomasi, (2012) "Mechanisms of Microstructure Control in Conventional Sintering - Sintering of Ceramics - New Emerging Techniques", Dr. Arunachalam Lakshmanan (Ed.), ISBN: 978-953-51-0017-1, InTech.
- [54] H. Yoshida, K. Hiraga and T. Yamamoto, "Densification behavior of Ti-doped polycrystalline alumina in a nitrogen-hydrogen atmosphere", *Materials Transactions*, 50 (2009), 1032-1036.